Synthesis and characterization of latex nanoparticles using a visible-light photoinitiating system in reverse micelles

Ernesto Maximiliano Arbeloa, Gabriela Valeria Porcal, Sonia Graciela Bertolotti & Carlos Mario Previtali

Colloid and Polymer Science
Kolloid-Zeitschrift und Zeitschrift für Polymere

ISSN 0303-402X
Volume 293
Number 2

Colloid Polym Sci (2015) 293:625-632
DOI 10.1007/s00396-014-3453-z

Springer

Colloid Polym Sci (2015) 293:625–632
DOI 10.1007/s00396-014-3453-z

SHORT COMMUNICATION

Synthesis and characterization of latex nanoparticles using a visible-light photoinitiating system in reverse micelles

Ernesto Maximiliano Arbeloa · Gabriela Valeria Porcal · Sonia Graciela Bertolotti · Carlos Mario Previtali

Received: 21 August 2014 / Revised: 23 October 2014 / Accepted: 6 November 2014 / Published online: 21 November 2014

Abstract This work shows the feasibility of using the photoinitiating system composed by the xanthene dye Eosin-Y and triethanolamine on the polymerization of acrylamide in benzyl-hexadecyl-dimethylammonium chloride (BHDC) reverse micelles. Molecular weights of polyacrylamide (MW_{PAA}) in the order of 10^5 and conversions up to 90 % are obtained. The size of the latex particles is in the range of the nanometers (d<50 nm). The effect of water content and concentrations of surfactant, amine, dye, and monomer on the particle size and MW_{PAA} are examined. Only the amine and monomer concentrations affect the MW_{PAA}. These results are interpreted on the basis of an exchange mechanism between micelles. Practically no effect on hydrodynamic diameters is observed when the value of MW_{PAA} is doubled. This is ascribed to a supercoiled structure of PAA inside of micelles. Our results also suggest that the polymer properties can be modulated by appropriate combination of the dye/surfactant electrical charges.

Keywords Dyes/pigments · Dynamic light scattering · Nanoparticles · Photopolymerization · Reverse micelles

Introduction

Microemulsions are transparent liquid systems consisting of at least ternary mixtures of oil, water, and surfactant. Sometimes, a cosurfactant is needed for the formation of a thermodynamically stable microemulsion. A transparent microemulsion is, in fact, heterogeneous (nanostructured) on a molecular scale. It is important to recognize that these systems are dynamic because micelles frequently collide via random Brownian motion. Microemulsion domains fluctuate in size and shape and undergo spontaneous coalescence to form dimers, which may exchange contents and then break apart again [1].

Due to the enormous inner surfaces of the nanostructures of water-in-oil (W/O) and oil-in-water (O/W) globular microemulsions (micelles), they can provide novel reaction sites for some inorganic/organic reactions and polymerizations. Microemulsion polymerization is an effective approach for preparing nanosized polymer particles and has attracted significant attention [2, 3]. The size of the particles can be controlled by the size of the microdroplets in the W/O microemulsions [4–6]. This is a very important topic with many potential applications in drug delivery, microencapsulation, etc. For this reason, a considerable amount of activity has been conducted in this area [7, 8].

Previous studies on polymerization in microemulsions mostly employed azobis-isobutyronitrile (AIBN) or persulfate as a photochemical UV or thermal initiator. Candau and coworkers were the first to study the polymerization of acrylamide in inverse microemulsions stabilized by sodium bis-2-ethyl-hexylsulfosuccinate (AOT) [9, 10]. They found that the particle sizes of the final microlatexes were in the order of nanometers (d~20–40 nm) and were larger than those of the initial monomer-swollen droplets (d~5–10 nm). Due to the low size dispersion and high molecular weights obtained, the authors concluded that each latex particle contained only a few polymer chains highly collapsed.

However, the use of radiation in the visible region presents several advantages compared to thermal or UV initiation of polymerization [11–14]. These advantages are, for example, (i) lower cost by making use of visible photons emitted by the Hg lamps which are lost when the light is only absorbed by a UV photoinitiator (PI), (ii) a better matching of the emission spectrum of the light source and the absorption spectrum of the PI when laser lights are used, (iii) higher penetration ability

E. M. Arbeloa (✉) · G. V. Porcal · S. G. Bertolotti · C. M. Previtali
Departamento de Química, Universidad Nacional de Río Cuarto, 5800 Río Cuarto, Córdoba, Argentina
e-mail: earbeloa@exa.unrc.edu.ar

of the visible radiation, and (iv) the opportunity to use sunlight for the curing of outdoor coatings.

The most common photoinitiator systems for vinyl polymerization in the visible are composed by a dye and an amine as an electron donor. In our laboratory, we have been interested for many years in the mechanistic aspects of PI systems operating in the visible. By means of laser-flash photolysis, we found that the photoinitiation mechanism involves an electron transfer from the co-initiator to the triplet state of the dye [15–19]. Active radicals derived from the amine are the responsible for initiating the polymerization.

Carver et al. employed a mixture of methylene blue/eosin/triethanolamine in the polymerization of acrylamide in AOT reverse micelles [20]. The authors obtained polymers with molecular weights in the same order with those obtained with thermal initiators. However, they did not take into account that the electrostatic interactions may affect the relative localization of the dyes in the interface region. This is a relevant aspect because a different proximity between dyes and amine might modify the polymer properties in a straightforward manner. Also, an efficient polymerization was found to occur under visible light by using $Ru(bpy)_3^{2+}$ or eosin as a sensitizer in O/W microemulsions containing cetyl-trimethylammonium persulfate as electron donor [21].

Recently, we reported the photopolymerization of acrylamide in reverse micelles of benzyl-hexadecyl-dimethylammonium chloride (BHDC), employing as photoinitiating system Safranine-O and triethanolamine (TEOA) [22]. The positively charged dye Safranine-O is localized in the interface region of BHDC reverse micelles, comicellizing with surfactant molecules and the co-initiator is in the water pool [23]. Small nanoparticles of polyacrylamide are formed with a low polydispersity and a molecular weight close to 10^6.

In the presence of electron donors such as tertiary amines, the negatively charged dye Eosin-Y (Eos) has been described as an efficient photoinitiator for the free radical polymerization of several monomers in homogeneous medium [24–29]. This PI has been used as an efficient photoinitiator for surface modification by surface-mediated polymerization [30]. In a comparative study of the efficiency of several xanthene dyes, Eos was among the most effective to initiate vinyl polymerization of acrylamide [19]. Furthermore, the Eos/tertiary amine system was found to initiate polymerization despite the presence of an excess of several inhibitors of radical polymerizations [31].

In a recent work, we published a study on the photophysics of Eos in AOT and BHDC reverse micelles [32]. In these microemulsions, the triplet state of the dye lives longer than in the homogeneous solvent. We conclude that this result is due to compartmentalization effect that suppresses the self-quenching process. Furthermore, a high efficiency of triplet quenching was achieved with an amine concentration much lower than that in the homogeneous solution. We ascribed to the closeness of both reactants this enhanced efficiency of the triplet quenching, because the dye localizes in the interface and the hydrophilic TEOA in the water pool of reverse micelles. In turn, a higher yield of radicals was found in BHDC than in AOT reverse micelles, which was attributed to the electrostatic interactions between surfactant and reactant molecules. Such results suggest that the Eos/TEOA/BHDC system may be suitable for initiating vinyl polymerizations in microemulsions.

In this work, we present the study on the polymerization of acrylamide in reverse micelles of BHDC, photoinitiated by Eosin-Y and triethanolamine (Scheme 1). The effect of the charge and localization of Eos in the reverse micelles on the polymer properties was assessed. It was of particular interest to investigate the factors that affect the properties of polymeric particles obtained by this visible-light initiating system and compared them with those previously reported on Safranine-O. Thus, the effect of variables such as water content and concentrations of dye, amine, surfactant, and monomer on molecular weight of the polymer and size of the particles was evaluated.

Materials and methods

Materials

Eosin-Y (Eos, 93 % of purity) was obtained from Aldrich and used without further purification. BHDC (Sigma) was two times recrystallized from ethyl acetate and dried under vacuum. Benzene and methanol were purchased from Sintorgan (HPLC grade) and used as received. Triethanolamine (TEOA) was commercially available and purified by standard procedures. Water was purified through a Millipore Milli-Q system. Acrylamide (AA, 99+%) and *N*,*N*′-methylene-bis-acrylamide (bis-AA, 99 %) were provided by Aldrich and used as received.

Preparation of polymeric nanoparticles

Reverse micelle solutions were prepared by dissolving the surfactant in the benzene and adding pure water to the desired water content ($w=[H_2O]/[surfactant]$). The stability of microemulsions composed by BHDC in a series of organic solvents, as well as for other homologous surfactants, has been studied at several water/surfactant ratios [33]. The authors interpreted their results in terms of two main effects: the curvature of the surfactant film separating the oil and water (interface) and the attractive interactions among water droplets [34]. Based on this model, the stabilization of W/O microemulsions would be due to the compromise between these two opposite effects. Beyond a certain threshold value of water content, the emulsion becomes unstable and an opalescence characteristic of phase

Scheme 1 Molecular structures of **a** Eosin-Y (Eos), **b** triethanolamine (TEOA), **c** acrylamide (AA), and **d** polyacrylamide (PAA)

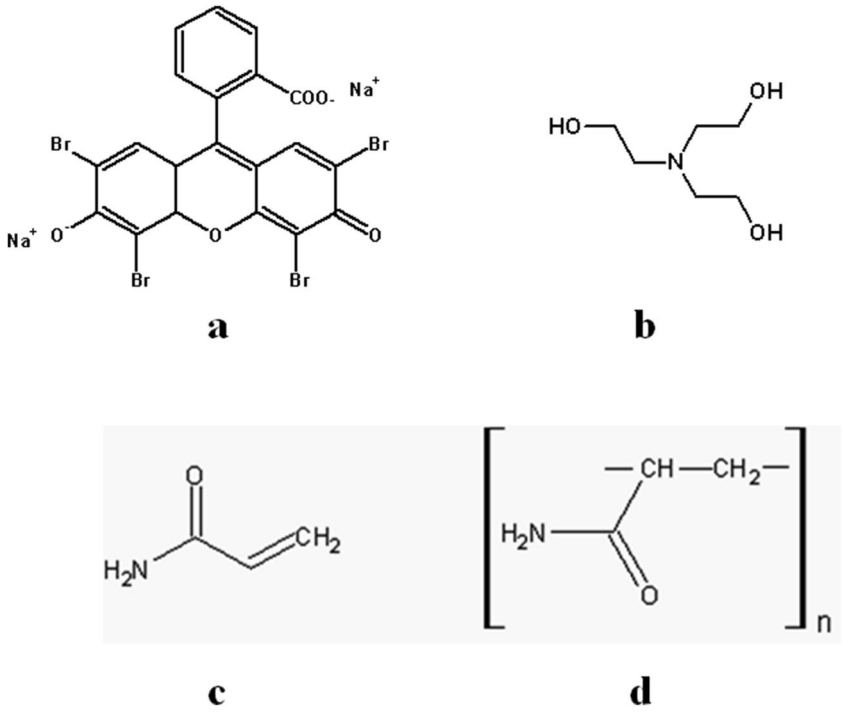

separation is promptly observed. In this case, all microemulsions remained stable and optically clear after adding water to *w* values desired (see Table 2 later).

A small amount of the dye dissolved in water was added to a final analytical concentration in the order of 10^{-6} M (Abs~ 0.15–0.2 at 532 nm). A suitable amount of co-initiator TEOA dissolved in water was also incorporated into micelles. The monomer (AA) and the crosslinker (bis-AA) were dissolved in the reverse micelles, aided by sonication, to the required concentration. In the crosslinking experiments, a ~4 % in weight of AA was replaced by bis-AA.

Previous to irradiation, solutions were deoxygenated by bubbling with organic solvent-saturated high-purity Ar for 30 min. The polymerization was carried out with a home-made photoreactor, by irradiation with eight green LEDs (λ_{max}=532 ±10 nm) at room temperature (~25 °C). Previous to polymerization, the reverse micelle solutions had a slightly pink coloration. The irradiation continued until the solution became colorless. After irradiation, all microemulsions remained stable and clear.

Particle size determination

The sizes of the latex particles were determined by dynamic light scattering (DLS). Nanoparticles remain disperse in the BHDC microemulsion, which was directly used for particle size determination. The solutions were diluted only when necessary, i.e., when the number of counts in the detector exceeded the instrumental limit. The hydrodynamic diameter and size distribution of particles was measured by using a Malvern 4700 goniometer and 7132 correlator with an argon-ion laser operating at 488 nm. All measurements were made at a scattering angle of 90° at temperature of 25 °C. The measurements were carried out by triplicate, and the results were analyzed with Zetasizer software (provided by the manufacturer).

Molecular weight determination

Polyacrylamide (PAA) was precipitated with an excess of methanol for molecular weight determination. The precipitate was separated by centrifugation and washed several times with methanol to remove residual monomer and with benzene to remove the surfactant. The polymer was then dried in a vacuum oven at 25 °C and allowed to stand in a desiccator for 24 h.

The molecular weights of PAA polymers were obtained by means of viscosimetry. A set of solutions of different concentrations was prepared by dissolving the dried PAA in water. The intrinsic viscosities (η) of these aqueous solutions were determined by using a Cannon-Fenske (Ostwald modified) viscosimeter. Molecular weights were obtained from Mark–Houwink–Sakurada equation [35, 36].

$$\eta = 0.01\ \mathrm{PM}^{0.755} \quad (1)$$

Results and discussion

The effect of the composition of the microemulsion on the yield and properties of latex nanoparticles was investigated. The molecular weights of polyacrylamide (MW_{PAA}) and

average hydrodynamic diameters of the latex particles (Z_{AVE}) obtained in each experiment are collected on Tables 2 and 4, respectively.

With the aim of elucidating the effect of the compartmentalization on AA polymerization, two experiments were conducted simultaneously. A microemulsion assay in BHDC 0.1 M/benzene at *w* 5 and a bulk water assay at pH 9 were carried out to the same co-initiator and monomer analytical concentrations (3×10^{-3} M and 0.15 M, respectively). At pH 9, it can be considered that the dominant species of the dye is the dianionic form [37]. In BHDC reverse micelles, a redshifted absorption spectrum of the dianionic form of Eos was recorded [32]. The Eos absorbances in both experiments were matched at 532 nm (Abs ~ 0.13).

Due to the short excited singlet lifetime of the dye and the TEOAconcentration employed, the triplet state of the dye is the species that generates the amino radical responsible for photoinitiating the polymerization. The fraction of triplets intercepted by the quencher may be calculated by the following:

$$f_T = \frac{k_q[\mathrm{TEOA}]}{k_0 + k_q[\mathrm{TEOA}]} \quad (2)$$

where k_0 and k_q are the quenching rate constants of Eos triplet in the absence and in the presence of the quencher TEOA, respectively.

According to (2) and due to the long lifetimes of the triplet state of Eos in both media, more than 90 % of triplets were quenched at the TEOA concentration used (see Table 1).

The microemulsion became colorless after 15 min of irradiation, whereas the water solution showed coloration of slightly yellowing. In the latter, no further changes were observed even by extending the irradiation time for 10 min more. By the addition of methanol to the irradiated microemulsion, a high molecular weight polymer (in the order of 10^5) with a high conversion (~80 %) was obtained. Since the dye was mainly located on the interface region [32], and co-initiator TEOA was present in the aqueous core, AA polymerization took place within the aqueous core of reverse micelles. On the other hand, a slight opalescence was observed by the addition of methanol to the aqueous solution.

Table 1 Fraction of triplets of Eos intercepted by TEOA 3×10^{-3} M in BHDC/benzene and water media

Medium	$^3\tau$ (μs)[a]	k_0 (s^{-1})	k_q (M^{-1} s^{-1})	f_T (%)
BHDC 0.1 M (*w* 5)	170	5.9×10^3	1.9×10^{7}[b]	~91
Water (pH 9)	120	8.3×10^3	4.2×10^{7}[c]	~94

[a] Lifetimes of the triplet state of Eos measured for this work

[b] Ref. [32]

[c] Ref. [19]

It was not possible to obtain a precipitate from the latter solution even by centrifuging at 4000 rpm. In a previous work, we reported on the PAA formation in aqueous solution from AA concentration 4-fold higher and TEOA concentration 6-fold higher than in the present work [19]. Thus, our results suggest that at the same experimental conditions, confinement effect increases the local concentration of AA in the water pool of reverse micelles, allowing further growth of the chains before the termination takes place. Whereas in aqueous solution the termination reactions are by bimolecular recombination, in reverse micelles, the growing chains are isolated from each other, preventing the bimolecular termination. Since the aggregation number of BHDC in benzene at w=10 is ca. 300 [38], at the surfactant concentration used here, the mean occupation number of the dye was less than 0.03 or less than 0.06 (Exps. #1 and #2 on Table 2, respectively). This makes it unlikely that there is more than one dye molecule per micelle, so the initiation of the polymer chain takes place in a very small fraction of the reverse micelles. It has been previously proposed that in microemulsions the chain growth is most likely governed by an exchange mechanism driven by coalescence of the micelles [4]. According to this mechanism, molecules solubilized in the aqueous core of reverse micelles would be redistributed over the micelles when they coalesce to form temporary dimmers, before breaking apart again [39]. The high molecular weights of polyacrylamide (MW_{PAA}) obtained in BHDC reverse micelles (see Table 2) suggests that primary radicals are very unlikely to enter a previously nucleated micelle to terminate polymerization. Therefore, according to the data collected on Table 2, the exchange of AA among water pools is the principal event and must take place several times before termination.

From photophysical characterization of Eos in BHDC reverse micelles [32], and the results discussed above, the following detailed mechanism may be proposed for the photopolymerization of AA in microemulsion systems:

$$\mathrm{Eos}^{2-} + h\nu \rightarrow {}^3\mathrm{Eos}^{2-}$$

$${}^3\mathrm{Eos}^{2-} + \mathrm{TEOA} \rightarrow \mathrm{Eos}^{3\bullet-} + \mathrm{TEOA}^{\bullet+} (\text{Intramicellar quenching})$$

$$\mathrm{TEOA}^{\bullet+} + \mathrm{AA} \rightarrow \mathrm{R}_1 (\text{Intramicellar initiation step})$$

$$\mathrm{R}_1 + \mathrm{AA} \rightarrow \mathrm{PAA} (\text{Intermicellar chain propagation})$$

As it can be seen in Table 1, MW_{PAA} presents only dependency on the monomer and co-initiator concentrations. The molecular weight is approximately doubled by doubling the AA concentration. Similar effect was observed on MW_{PAA} as TEOA was reduced to half its initial concentration. On the other hand, no significant differences in MW_{PAA} were found as a function of the Eos concentration, aqueous pool size (given by *w*), or amount of micelles (given by BHDC concentration).

Table 2 Molecular weights of PAA (MW_{PAA}) determined by viscosimetric measurements under several experimental conditions. All concentrations are expressed in moles per liter

Exp. #	BHDC	*w*	Eos/10^{-6}	TEOA/10^{-3}	AA	$MW_{PAA}/10^{5a}$	Conversion (%)
1	0.1	5	1.4	3	0.15	2.9	~85–90
2	0.1	5	2.8	3	0.15	2.7	~85–90
3	0.1	5	1.4	1.5	0.15	4.5	~85–90
4	0.1	5	1.4	3	0.075	1.6	~90
5	0.05	5	1.4	3	0.075	1.4	~90
6	0.1	10	1.4	3	0.075	1.4	~90

[a] Estimated error: $\pm 0.2 \times 10^5$

Similar results were reported by Carver et al. [20] on polymerization of AA in AOT reverse micelles, using a mixture of dyes and TEOA as initiator system. Modifying the concentrations of this mixture, they observed that MW_{PAA} was independent of the rate of polymerization. They concluded that such results may be due to a degradative chain transfer mechanism, which leads to first-order termination in radical concentration. As explained above, in BHDC reverse micelles, growing radicals are isolated from other growing radicals, and therefore bimolecular recombination is an improbable way of termination. Therefore, the high MW_{PAA} obtained ($2–3 \times 10^5$), considering that initial monomer units per micelle were 400–500 on average (ca. 3×10^4), supports the monoradical route to be the predominant mode of termination.

Similarly, no changes in MW_{PAA} were observed when the surfactant concentration was reduced to half at constant *w*. This seems reasonable since the amount of reverse micelles decreased but the mean occupation number of the dye yet remained too low. This situation is analogous to increase Eos concentration and reinforces the explanation based on the exchange mechanism given. Likewise, polymerization driven by an exchange mechanism would explain why the molecular weight was approximately reduced to the half when AA concentrations were made twice lower (compare Exps. #1 and #4 on Table 2).

Table 2 shows that a 2-fold increase in the size of the micelles (*w*) did not show appreciable differences on MW_{PAA}. This suggests that, at constant monomer concentration, the growth of the polymer chain does not depend on the volume available within the micelle. Indeed, the chain extension is limited by the feasibility of termination reactions that may occur. And the latter is a function only of the occupation number of the dye and the amine concentration, as explained earlier. Otherwise, it would have achieved a higher MW_{PAA} at $w=10$, due to a more spacious microenvironment.

Table 2 also show that MW_{PAA} increases when TEOA concentration decreases (compare Exps. #1 and #3). Because there are three molecules of TEOA per micelle on average, the amine might be acting as a chain transfer agent as well as a reducing agent for the dye [20]. The probability that this reaction occurs decreases as the concentration of amine decreases, yielding higher MW_{PAA}.

At constant AA concentration, a higher MW_{PAA} involves a lower number of latex particles per occupied micelle. This number can be estimated making use of the model proposed by Candau et al. [9] according to the following equation:

$$n = \frac{4}{3}\pi(R_H - \ell_{BHDC})^3 \frac{\rho_{PAA} N_A}{MW_{PAA}} \quad (3)$$

where R_H is the hydrodynamic radius of the micelles (see Table 4); $\ell_{BHDC}=25.5$ Å corresponds to the length of the surfactant [38]; $\rho_{PAA}=1.399$ g/cm^3 is the density of PAA polymer [9]; N_A is the Avogadro's number; and MW_{PAA} are the molecular weights listed in Table 2.

From (3), values of 22 and 12 particles per micelle for Exps. #1 and #3 (Table 2) were obtained, respectively. These results are in the order of magnitude to those reported by these authors [9]. The estimated numbers of particles per occupied micelle supports the idea proposed above that a lower probability of termination driven by a lower TEOA concentration leads to a higher MW_{PAA}.

Similar trends were reported by our group in a previous paper on photopolymerization of AA initiated by Safranine-O in BHDC reverse micelles [22]. In that work, no changes on MW_{PAA} were observed with an increase of *w*. Instead, a 2-fold increment in MW_{PAA} was recorded by doubling simultaneously the AA and the surfactant concentrations. Since we have concluded here that surfactant concentration has no effect on MW_{PAA}, we can attribute the increment in MW_{PAA} reported by Porcal et al. [22] only to the AA increment.

Table 3 compares the MW_{PAA} obtained with Eos and Safranine-O (Saf) in a determined set of experimental conditions. A priori, it would be expected that the higher the radical

Table 3 Comparison of the MW_{PAA} obtained by Eos or Saf mediated polymerization in BHDC 0.1 M/benzene at *w* 5

	Eos	Saf[a]
MW_{PAA}	3×10^5	1×10^6
Φ_R	0.024[b]	0.22
[TEOA] (mM)	3.00	0.75
[AA] (M)	0.15	
Occupation number	<3 %	
f_T	>90 %	

[a] Ref. [22]
[b] Ref. [32]

yield (Φ_R), the shorter the polymer chain length. However, the opposed situation is recorded on Table 3. As with both dyes the nucleated particles were less than 3 %, then the Φ_R is not a decisive parameter on MW_{PAA} in these reverse micelle systems.

It seems to be that the different proximity between both dyes and the amine would explain the difference in reactivity and MW_{PAA} obtained with Eos and Saf. The electrostatic repulsion between positively charged Saf and BHDC molecules directs the dye localized in the interface towards inside of the water pool, where TEOA is solubilized. Instead, the negatively charged Eos is deeper in the micellar interface and is further away from the amine. A 4-fold higher TEOA concentration with Eos than with Saf is required to obtain a similar triplet-intercepted fraction (f_T). This relative excess in TEOA concentration may promote more termination steps when using Eos, so reducing the chain length of the growing PAA. Therefore, we may conclude that the electrostatic interaction between dyes and surfactant molecules modulates the MW_{PAA}, due to a distinct location of the dyes in the interface region of BHDC reverse micelles.

The sizes of microemulsion droplets were analyzed by DLS, where the correlation functions recorded showed monomodal distributions. Thus, a cumulant algorithm was used to fit the correlograms to monoexponential decays [40, 41]. Figure 1 illustrates representative plots of DLS measurements for BHDC reverse micelles and the latex of PAA. This fitting method allows extracting the average hydrodynamic diameter values (Z_{AVE}) of the latex particles from experimental data. Another parameter that the algorithm computes is the polydispersity index (PI), which provides information about the width of the size distribution. The Z_{AVE} and PI values obtained in the present work are summarized on Table 4.

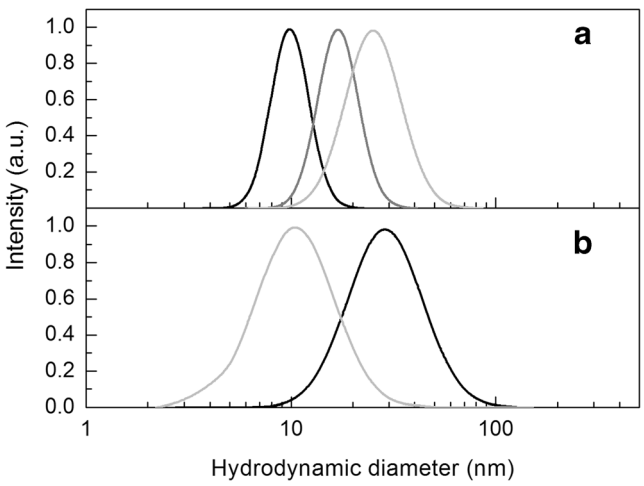

Fig. 1 Hydrodynamic diameter distributions of **a** empty micelles (*black curve*), micelles plus AA 0.075 M (*dark gray curve*), micelles plus AA 0.15 M (*gray curve*); and **b** latex nanoparticles expressed by intensity of scattered light (*black curve*) and by number of nanoparticles (*gray curve*)

Table 4 Average hydrodynamic diameter (Z_{AVE}) and the polydispersity index (PI) of the nanoparticles, obtained from cumulant analysis

Nanoparticles	Z_{AVE} (nm)[a]	PI[b]
RMs (w=5)	10.0	0.04
RMs+AA (0.075 M)	16.6	0.09
RMs+AA (0.15 M)	25.5	0.09
Latex (Exp. #1)[c]	28.7	0.18
Latex (Exp. #3)[c]	28.1	0.14
Latex (AA+bis-AA)	27.1	0.15

[a] Estimated error: ±0.1 nm

[b] Estimated error: ±0.01

[c] See Table 2

Figure 1a shows the intensity of scattered light by different reverse micelle systems as a function of the size. All size distribution curves are very narrow according to the low PI values reported on Table 4 and are centered in the corresponding Z_{AVE} values. In turn, although the polymerization broadens the size distribution, the PI remains at a small value (the limit of acceptance is 0.7). This means that the polymerization process in these systems yields latex particles mainly of a single size.

To highlight the consistency of the results, the size distribution of latex solution is represented by two equivalent plots in Fig. 1b. When the intensity of scattered light is plotted vs. the size of nanoparticles (commonly referred to as "distribution by intensity," black curve), the maximum of the curve corresponds to Z_{AVE} values reported in Table 4. It is expected that the highest percentage of scattered radiation is due to larger particles (i.e., latex nanoparticles), which are in smaller amount. The front of this curve corresponds to empty micelles, which scattered only a little fraction of the incident light. When the amount of nanoparticles is plotted as a function of their diameter (commonly referred to as "distribution by number," thin gray curve in Fig. 1b), the maximum Z_{AVE} is about 10 nm. Namely, the most of the nanoparticles corresponds to empty reverse micelles after polymerization. This is a consequence that polymerization took place only in a few nucleated micelles, according to the exchange mechanism proposed above. Really, it can be seen from the tail of this curve that only very few particles has a diameter around 20–30 nm.

Table 4 shows that Z_{AVE} values are in the range of tens of nanometer for all the systems evaluated. As it can be seen, the size of the reverse micelles is sensitive to the concentration of guest molecules in the aqueous core. The Z_{AVE} increases progressively with increasing concentration of AA. On the other hand, after polymerization, the hydrodynamic diameter of latex nanoparticles is practically independent of the MW_{PAA} obtained (compare Tables 2 and 4). Moreover, the Z_{AVE} is enlarged only ca. 3 nm even though the number of AA

units increased from 400–500 (monomeric form) to 3500–4000 (polymerized form) approximately.

These results seem to indicate a supercoiled structure of PAA inside of reverse micelles, such that the size of the droplets is unaffected by a longer chain. The supercoiling of PAA has been suggested to explain the obtaining of high MW_{PAA} inside a limited volume [9].

The values of the hydrodynamic diameter for the nanoparticles evaluated in the present work are in good agreement with those previously reported by our group, concerning the photopolymerization of AA in BHDC initiated by Saf/TEOA system [22].

In another experiment, some small amount (ca. 4 % in weight) of bis-AA was added to the microemulsion, while all other conditions were kept as the Exp. #1 (see Table 2). Bis-AA has the capability to undergo cyclization or multiple crosslinking reactions [42]. During the copolymerization between AA and bis-AA, pendant vinyl groups are created when bis-AA has partially reacted. Such pendant groups may then react with radicals on the same growing chain or with radicals on other chains linked to the growing crosslinked polymer. Table 4 shows the size parameters for latex containing crosslinked PAA. The narrow size distribution and the small diameter obtained indicate that this method is suitable for obtaining highly monodisperse crosslinked nanoparticles of PAA. Therefore, because nanoparticles based on crosslinked PAA are of particular interest as carriers of dyes in photodynamic therapy among other applications [43, 44], the results in the present work are relevant to contribute to the development of new nanotechnologies.

Conclusions

We have presented here a study on suitability of Eosin-Y/TEOA system to photoinitiate the AA polymerization in BHDC reverse micelles. This method allowed synthesizing thermodynamically stable nanoparticles with diameters of ca. 30 nm. The polyacrylamide molecular weights obtained were as high as ~$2–4\times10^5$. It was found that only monomer and amine concentrations may affect the chain length of the polymer. However, the particle size was substantially not affected by any of the experimental conditions tested. To explain these results, we have ascribed an exchange mechanism between the water pools of the reverse micelles as the driving force of polymerization process. According to the Z_{AVE} values obtained here, a supercoiled structure of the polymer is required to hold such a high molecular weight in such a small volume.

The results in the present work are in agreement with those previously reported by us with the Safranine-O/TEOA initiating system in BHDC reverse micelles. However, the specific localization of the dye in the interface modulates the polymer molecular weight. This location depends upon the relative electrical charges of the dye and the surfactant. A lower molecular weight results when the dye is of opposite charge and localizes deeper in the micellar interface. Irrespective of the dye used, the high conversions and the properties of the polymers obtained demonstrate the high efficiency of these visible-light initiators.

Both the polymer molecular weights and the particle sizes obtained here are comparable with those reported in microemulsions using thermal or UV initiators. Therefore, our investigation supports the applicability of these dye/amine initiator systems in the polymer and nanotechnology fields.

Acknowledgments Financial support from CONICET (PIP 2010–0284) and Universidad Nacional de Río Cuarto is gratefully acknowledged.

References

1. Friberg S, Bothorel P (1987) Microemulsions: structure and dynamics. CRC, Boca Raton
2. Pavel FM (2004) Microemulsion polymerization. J Dispers Sci Technol 25:1–16
3. Hentze H-P, Kaler EW (2003) Polymerization of and within self-organized media. Curr Opin Colloid Interface Sci 8:164–178
4. Munshi N, De TK, Maitra A (1997) Size modulation of polymeric nanoparticles under controlled dynamics of microemulsion droplets. J Colloid Interface Sci 190:387–391
5. Vakurov A, Pchelintsev NA, Forde J, Ó'Fágáin C, Gibson T, Millner P (2009) The preparation of size-controlled functionalized polymeric nanoparticles in micelles. Nanotechnol 20(295605):1–7
6. Rao JP, Geckeler KE (2011) Polymer nanoparticles: preparation techniques and size-control parameters. Prog Polym Sci 36:887–913
7. Eastoe J, Hollamby MJ, Hudson L (2006) Recent advances in nanoparticle synthesis with reversed micelles. Adv Colloid Interface Sci 128–130:5–15
8. Nimesh S, Manchanda R, Kumar R, Saxena A, Chaudhary P, Yadav V, Mozumdar S, Chandra R (2006) Preparation, characterization and in vitro drug release studies of novel polymeric nanoparticles. Int J Pharm 323:146–152
9. Candau F, Leong YS, Pouyet G, Candau S (1984) Inverse microemulsion polymerization of acrylamide: characterization of the water-in-oil microemulsions and the final microlatexes. J Colloid Interface Sci 101:167–183
10. Candau F, Leong YS, Fitch RM (1985) Kinetic study of the polymerization of acrylamide in inverse microemulsion. J Polym Sci: Polym Chem Ed 23:193–214
11. Grotzinger C, Burget D, Jacques P, Fouassier JP (2003) Visible light induced photopolymerization: speeding up the rate of polymerization by using co-initiators in dye/amine photoinitiating systems. Polym 44:3671–3677
12. Ibrahim A, Ley C, Tarzi OI, Fouassier JP, Allonas X (2010) Visible light photoinitiating systems: toward a good control of the photopolymerization efficiency. J Photopolym Sci Technol 23:101–108
13. Tarzi OI, Allonas X, Ley C, Fouassier JP (2010) Pyrromethene derivatives in three-component photoinitiating systems for free radical photopolymerization. J Polym Sci Part A: Polym Chem 48: 2594–2603

14. Zhang G, Song IY, Ahn KH, Park T, Choi W (2011) Free radical polymerization initiated and controlled by visible light photocatalysis at ambient temperature. Macromol 44:7594–7599
15. Previtali CM, Bertolotti SG, Neumann MG, Pastre IA, Rufs AM, Encinas MV (1994) Laser flash photolysis study of the photoinitiator system safranine t-aliphatic amines for vinyl polymerization. Macromol 27:7454–7458
16. Encinas MV, Rufs AM, Neumann MG, Previtali CM (1996) Photoinitiated vinyl polymerization by safranine T/triethanolamine in aqueous solution. Polym 37:1395–1398
17. Rivarola CR, Bertolotti SG, Previtali CM (2001) Polymerization of acrylamide photoinitiated by tris(2,2′-bipyridine)ruthenium(II)–amine in aqueous solution: effect of the amine structure. J Polym Sci Part A: Polym Chem 39:4265–4273
18. Gómez ML, Previtali CM, Montejano HA, Bertolotti SG (2007) Photoreaction and photopolymerization studies on phenoxazin dyes/diphenyliodonium chloride salt. J Photochem Photobiol A: Chem 188:83–89
19. Encinas MV, Rufs AM, Bertolotti SG, Previtali CM (2009) Xanthene dyes/amine as photoinitiators of radical polymerization: a comparative and photochemical study in aqueous médium. Polym 50:2762–2767
20. Carver MT, Dreyer U, Knoesel R, Candau F (1989) Kinetics of photopolymerization of acrylamide in AOT reverse micelles. J Polym Sci Part A: Polym Chem 27:2161–2177
21. Grätzel CK, Jirousek M, Grätzel M (1986) Photoredox-induced polymerization of microemulsion droplets. Langmuir 2:292–296
22. Porcal GV, Arbeloa EM, Chesta CA, Bertolotti SG, Previtali CM (2013) Visible light photopolymerization in BHDC reverse micelles. Laser flash photolysis study of the photoinitiating mechanism. J Photochem Photobiol A: Chem 257:60–65
23. Porcal GV, Arbeloa EM, Orallo DE, Bertolotti SG, Previtali CM (2011) Photophysics of safranine-O and phenosafranine in reverse micelles of BHDC. J Photochem Photobiol A: Chem 226:51–56
24. Fouassier JP, Chesneau E (1991) Polymérisation induite sous irradiation laser visible, 4. Le système éosine/photoamorceur ultra-violet/amine. Makromol Chem 192:245–260
25. Kumar SG, Neckers DC (1991) Laser-induced three-dimensional photopolymerization using visible initiators and UV cross-linking by photosensitive comonomers. Macromol 24:4322–4327
26. Mallavia R, Amat-Guerri F, Fimia A, Sastre R (1994) Synthesis and evaluation as a visible-light polymerization photoinitiator of a new Eosin ester with an *O*-benzoyl-α-oxooxime group. Macromol 27:2643–2646
27. Burget D, Fouassier JP, Amat-Gerri F, Mallavia R, Sastre R (1999) Enhanced activity as polymerization photoinitiators of Rose Bengal and Eosin esters with an *O*-benzoyl-α-oxooxime group: the role of the excited state reactivity. Acta Polym 50:337–346
28. Popielarz R, Vogt O (2008) Effect of coinitiator type on initiation efficiency of two-component photoinitiator systems based on Eosin. J Polym Sci Part A: Polym Chem 46:3519–3532
29. Neumann MG, Schmitt CC, Maciel H (2005) The photopolymerization of styrenesulfonate initiated by dyes. The effect of monomer aggregation. J Photochem Photobiol A: Chem 175:15–21
30. Avens HJ, Randle TJ, Bowman CN (2008) Polymerization behavior and polymer properties of eosin-mediated surface modification reactions. Polym 49:4762–4768
31. Avens HJ, Bowman CN (2009) Mechanism of cyclic dye regeneration during eosin-sensitized photoinitiation in the presence of polymerization inhibitors. J Polym Sci Part A: Polym Chem 47:6083–6094
32. Arbeloa EM, Porcal GV, Bertolotti SG, Previtali CM (2013) Effect of the interface on the photophysics of eosin-Y in reverse micelles. J Photochem Photobiol A: Chem 252:31–36
33. Jada A, Lang J, Zana R (1990) Ternary water in oil microemulsions made of cationic surfactants, water, and aromatic solvents. 1. Water solubility studies. J Phys Chem 94:381–387
34. Hou M-J, Shah DO (1987) Effects of the molecular structure of the interface and continuous phase on solubilization of water in water/oil microemulsions. Langmuir 3:1086–1096
35. Hosier IL, Vaughan AS, Mitchell GR, Siripitayananon J, Davis FJ (2004) Polymer characterization. In: Davis FJ (ed) Polymer chemistry. Oxford University Press, New York, pp 1–67
36. Gnanou Y, Fontanille M (2008) Determination of molar masses and study of conformations and morphologies by physical methods. In: Gnanou Y, Fontanille M (eds) Organic and physical chemistry of polymers. Wiley, Hoboken, pp 147–211
37. Levillain P, Fompeydie D (1985) Determination of equilibrium constants by derivative spectrophotometry. Application to the pK, s of Eosin. Anal Chem 57:2561–2563
38. Jada A, Lang J, Zana R, Makhloufi R, Hirsch E, Candau SJ (1990) Ternary water in oil microemulsions made of cationic surfactants, water, and aromatic solvents. 2. Droplet sizes and interactions and exchange of material between droplets. J Phys Chem 94:387–395
39. Bommarius AS, Holzwarth JF, Wang DIC, Hatton TA (1990) Coalescence and solubilizate exchange in a cationic four-component reversed micellar system. J Phys Chem 94:7232–7239
40. ISO (1996) Methods for determination of particle size distribution part 8: photon correlation spectroscopy. In: International Standard ISO13321. International Organisation for Standardisation (ISO)
41. Dahneke BE (1983) Measurement of suspended particles by quasi-elastic light scattering. Wiley, Minnesota
42. Naghash HJ, Okay O (1996) Formation and structure of polyacrylamide gels. J Appl Polym Sci 60:971–979
43. Gao D, Agayan RR, Xu H, Philbert MA, Kopelman R (2006) Nanoparticles for two-photon photodynamic therapy in living cells. Nanolett 6:2383–2386
44. Gao D, Xu H, Philbert MA, Kopelman R (2007) Ultrafine hydrogel nanoparticles: synthetic approach and therapeutic application in living cells. Angew Chem Int Ed 46:2224–2227